Electronic Supporting Information (ESI)

Two semiconductive haloargentates with metal-complex cations: Crystal structures, band gaps, photocurrent responses and theoretical investigations

*Shu-Yue Xie,[a] Ming-Hui Liu,[a] Ning Wang,[a] Xi-Meng Zhang,[a] Shen-Hao Wang,[a] Yan Yang,[ab] Jun Li,[*ab] and Bo Zhang[*ab]*

[a]*College of Chemistry and Chemical Engineering, Liaocheng University, Liaocheng 252059, China*
[b]*State Key Laboratory of Structural Chemistry, Fujian Institute of Research on the Structure of Matter, Chinese Academy of Sciences, Fuzhou 350002, China*

[*]*E-mail: junli@lcu.edu.cn; bzhang@lcu.edu.cn*

Contents

1. Selected bond lengths and bond angles

Table S1 Selected bond lengths (Å) and bond angles (°) for compound **1**.

Ag(1)−I(3)	2.7309(9)	Co(1)−N(2)	2.108(8)
Ag(1)−I(2)	2.7776(12)	Co(1)−N(2)#4	2.108(8)
Ag(1)−I(2)#1	2.8438(12)	Co(1)−N(2)#5	2.108(8)
Ag(1)−I(1)	2.9439(13)	Co(1)−N(1)#5	2.098(8)
I(2)−Ag(1)#2	2.8438(12)	Co(1)−N(1)	2.098(8)
I(3)−Ag(1)#3	2.7309(9)	Co(1)−N(1)#4	2.098(8)
I(1)−Ag(1)#1	2.9440(13)	I(1)−Ag(1)#2	2.9440(13)
Ag(1)−Ag(1)#1	2.9963(15)	Ag(1)−Ag(1)#2	2.9964(15)
I(3)−Ag(1)−I(2)	119.43(4)	N(2)#5−Co(1)−N(1)#5	77.0(3)
I(3)−Ag(1)−I(2)#1	101.44(3)	N(2)−Co(1)−N(1)	77.0(3)
I(2)−Ag(1)−I(2)#1	113.10(5)	N(2)#4−Co(1)−N(1)	91.0(3)
I(3)−Ag(1)−I(1)	100.21(3)	N(2)#5−Co(1)−N(1)	170.7(3)
I(2)−Ag(1)−I(1)	111.69(3)	N(1)#5−Co(1)−N(1)	96.1(3)
I(2)#1−Ag(1)−I(1)	109.80(3)	N(2)−Co(1)−N(1)#4	170.7(3)
N(2)−Co(1)−N(2)#4	96.6(3)	N(2)#4−Co(1)−N(1)#4	77.0(3)
N(2)−Co(1)−N(2)#5	96.6(3)	N(2)#5−Co(1)−N(1)#4	91.0(3)
N(2)#4−Co(1)−N(2)#5	96.6(3)	N(1)#5−Co(1)−N(1)#4	96.1(3)
N(2)−Co(1)−N(1)#5	90.9(3)	N(1)−Co(1)−N(1)#4	96.1(3)
N(2)#4−Co(1)−N(1)#5	170.7(3)		

Symmetry transformations used to generate equivalent atoms: #1 −*y*+1, *x*−*y*, z; #2 −*x*+*y*+1, −*x*+1, *z*; #3 −*x*+5/3, −*y*+1/3, −*z*+1/3; #4 −*x*+*y*+2, −*x*+1, *z*; #5 −*y*+1, *x*−*y*−1, *z*.

Table S2 Hydrogen bonds (Å) and angles (º) for compound **1**.

D−H···A	d(D−H)	d(H···A)	d(D···A)	<(DHA)
N(3)−H(3A)···I(2)#1	0.89	3.27	3.6903(9)	111.6
N(3)−H(3A)···I(2)#6	0.89	3.21	3.6903(9)	116.6
N(3)−H(3B)···I(2)#7	0.89	2.84	3.6903(9)	160.2
N(3)−H(3C)···I(2)#2	0.89	2.97	3.6903(9)	139.5
N(3)−H(3D)···I(2)	0.89	2.8	3.6903(9)	180
C(2)−H(2)···I(3)	0.93	3.07	3.928(12)	154.9

Symmetry transformations used to generate equivalent atoms: #1 −*y*+1, *x*−*y*, z; #2 −*x*+*y*+1, −*x*+1, *z*; #6 *x*−*y*+1/3, *x*−1/3, −*z*+2/3; #7 *y*+1/3, −*x*+*y*+2/3, −*z*+2/3.

Table S3 Selected bond lengths (Å) and bond angles (°) for compound **2**.

Ag(1)−Br(2)	2.5805(5)	Br(3)−Ag(1)#2	2.8143(8)
Ag(1)−Br(1)	2.6323(7)	Ni(1)−N(2)#1	2.054(4)
Ag(1)−Br(1)#1	2.7082(7)	Ni(1)−N(2)#2	2.054(4)
Ag(1)−Br(3)	2.8144(8)	Ni(1)−N(2)	2.054(4)
Br(3)−Ag(1)#1	2.8143(8)	Ni(1)−N(1)#1	2.078(4)
Br(1)−Ag(1)#2	2.7083(7)	Ni(1)−N(1)	2.078(4)
Br(2)−Ag(1)#3	2.5805(5)	Ni(1)−N(1)#2	2.078(4)
Ag(1)−Ag(1)#1	3.0384(8)	Ag(1)−Ag(1)#2	3.0384(8)

Br(2)−Ag(1)−Br(1)	124.84(2)	N(2)−Ni(1)−N(1)#1	171.18(15)
Br(2)−Ag(1)−Br(1)#1	101.94(2)	N(2)#1−Ni(1)−N(1)	91.37(14)
Br(1)−Ag(1)−Br(1)#1	110.64(3)	N(2)#2−Ni(1)−N(1)	171.18(15)
Br(2)−Ag(1)−Br(3)	102.083(18)	N(2)−Ni(1)−N(1)	78.29(14)
Br(1)−Ag(1)−Br(3)	109.02(2)	N(1)#1−Ni(1)−N(1)	95.46(13)
Br(1)#1−Ag(1)−Br(3)	106.87(2)	N(2)#1−Ni(1)−N(1)#2	171.18(15)
N(2)#1−Ni(1)−N(2)#2	95.50(14)	N(2)#2−Ni(1)−N(1)#2	78.29(14)
N(2)#1−Ni(1)−N(2)	95.50(14)	N(2)−Ni(1)−N(1)#2	91.37(14)
N(2)#2−Ni(1)−N(2)	95.50(14)	N(1)#1−Ni(1)−N(1)#2	95.45(13)
N(2)#1−Ni(1)−N(1)#1	78.29(14)	N(1)−Ni(1)−N(1)#2	95.45(13)
N(2)#2−Ni(1)−N(1)#1	91.37(14)		

Symmetry transformations used to generate equivalent atoms: #1 −*x*+*y*+1, −*x*+1, *z*; #2 −*y*+1, *x*−*y*, *z*; #3 −*x*+2, −*y*+1, −*z*.

Table S4 Hydrogen bonds (Å) and angles (°) for compound **2**.

D−H···A	d(D−H)	d(H···A)	d(D···A)	<(DHA)
N(3)−H(3A)···Br(1)#2	0.88	2.86	3.5770(7)	139.7
N(3)−H(3A)···Br(1)#1	0.88	3.12	3.5770(7)	114.4
N(3)−H(3B)···Br(1)#4	0.88	3.12	3.5770(7)	114.4
N(3)−H(3B)···Br(1)#5	0.88	2.86	3.5770(7)	139.7
N(3)−H(3C)···Br(1)#6	0.9	2.92	3.5770(7)	131.7
N(3)−H(3D)···Br(1)	0.9	2.77	3.5770(7)	150.5
C(9)−H(9)···Br(2)#2	0.93	2.82	3.702(5)	159.5

Symmetry transformations used to generate equivalent atoms: #1 −*x*+*y*+1, −*x*+1, *z*; #2 −*y*+1, *x*−*y*, *z*; #4 −*x*+4/3, −*y*+2/3, −*z*−1/3; #5 *x*−*y*+1/3, *x*−1/3, −*z*−1/3; #6 *y*+1/3, −*x*+*y*+2/3, −*z*−1/3.

2. Crystal structure

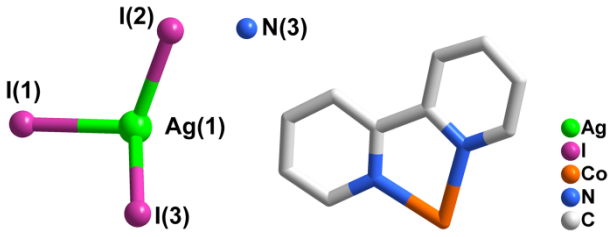

Fig. S1 The asymmetric unit of compound **1**.

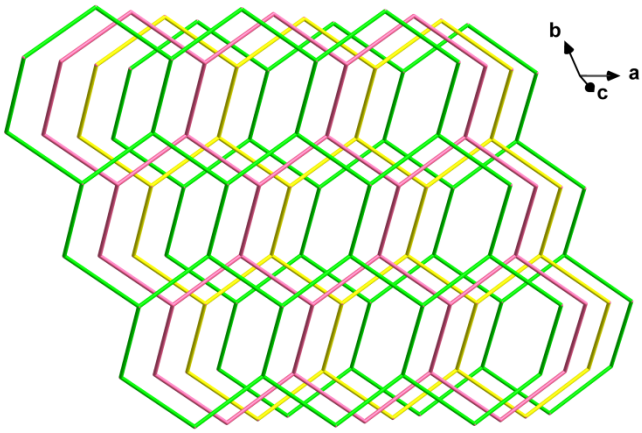

Fig. S2 The $\{6^3\}$ topology of title compounds.

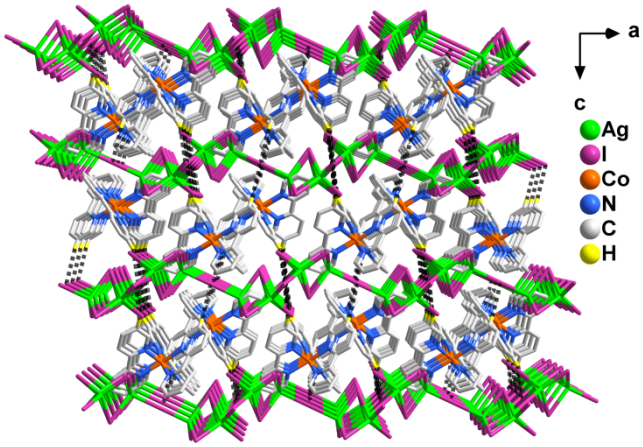

Fig. S3 Perspective view of compound **1** along the *b* axis, in which the dashed line represents the C−H···I hydrogen bond interactions.

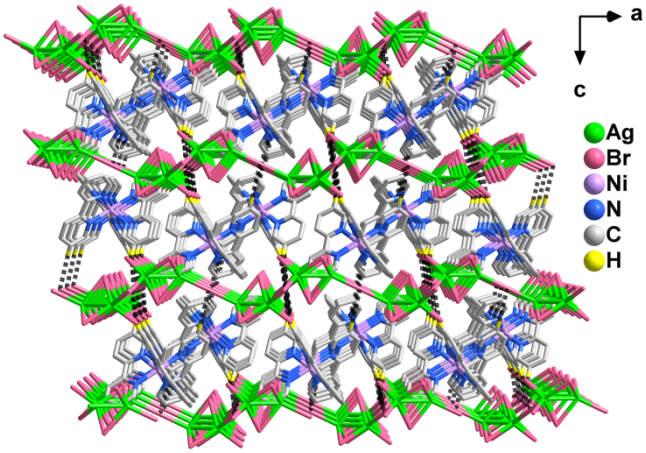

Fig. S4 Perspective view of compound **2** along the *b* axis, in which the dashed line represents the C−H···Br hydrogen bond interactions.

3. Hirshfeld surface

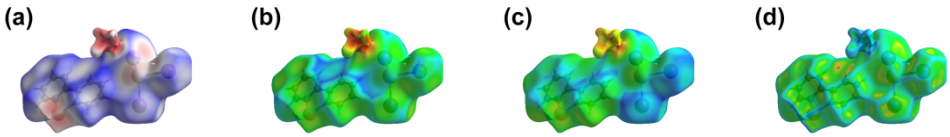

Fig. S5 Hirshfeld surface analyses mapped with d_{norm} (a), d_e (b), d_i (c), and curvedness (d) for compound **1**.

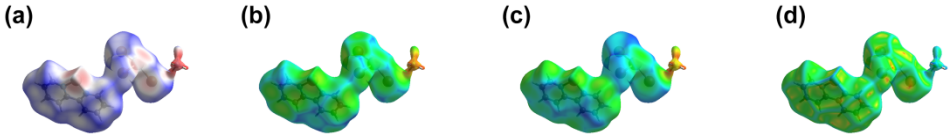

Fig. S6 Hirshfeld surface analyses mapped with d_{norm} (a), d_e (b), d_i (c), and curvedness (d) for compound **2**.

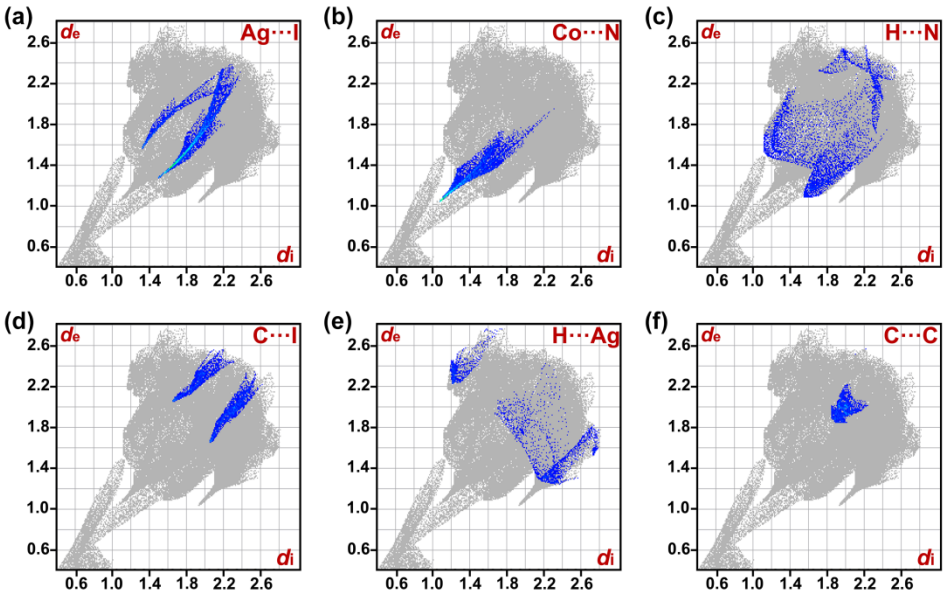

Fig. S7 Fingerprint plots: resolved into Ag···I (a), Co···N (b), H···N (c), C···I (d), H···Ag (e), and C···C (f) contacts for compound **1**.

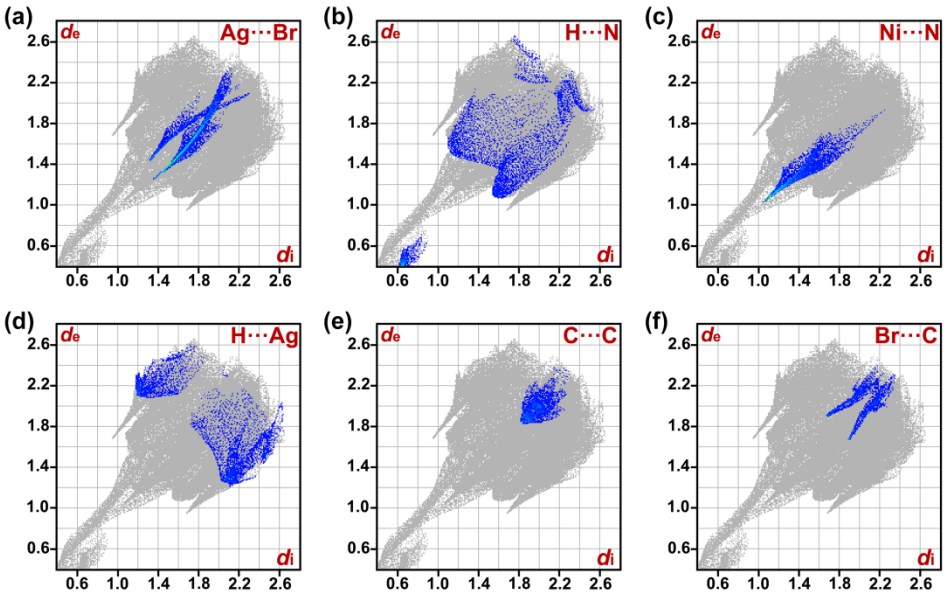

Fig. S8 Fingerprint plots: resolved into Ag···Br (a), H···N (b), Ni···N (c), H···Ag (d), C···C (e), and Br···C (f) contacts for compound **2**.

4. Physical measurements

4a). EDX

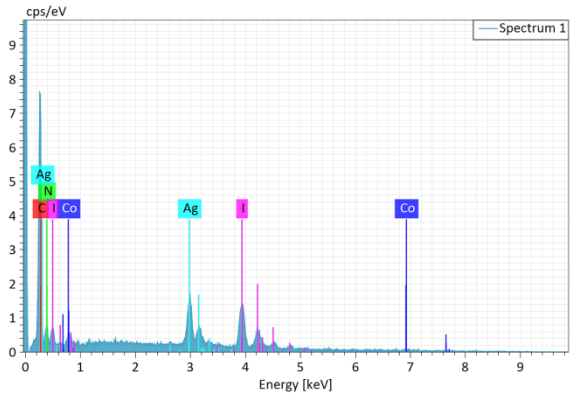

Fig. S9 EDX spectrum of compound **1**.

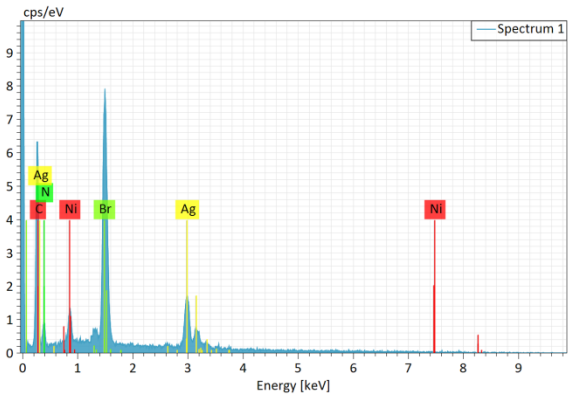

Fig. S10 EDX spectrum of compound **2**.

4b). XPS

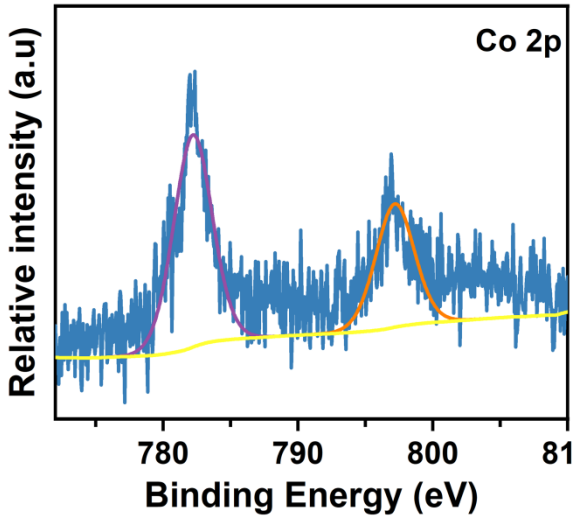

Fig. S11 High-resolution Co-2p spectrum of compound **1**.

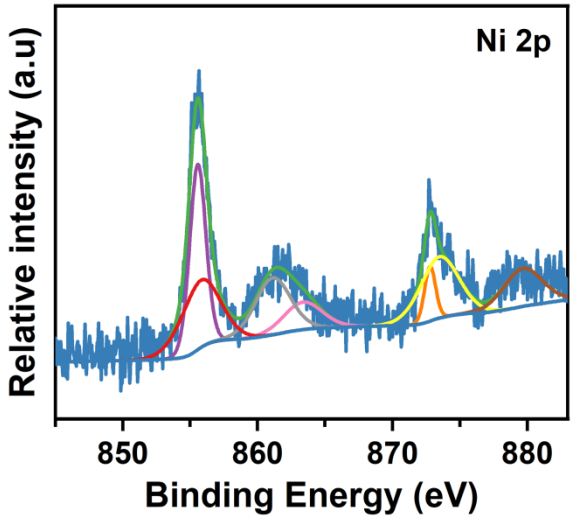

Fig. S12 High-resolution Ni-2p spectrum of compound **2**.

5. DFT calculation

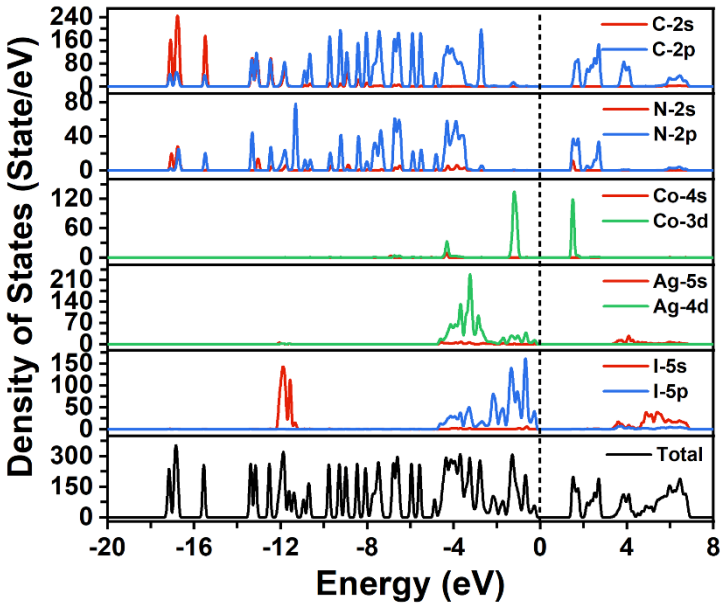

Fig. S13 The total density of states and partial density of states of compound **1**. The valence-band maximum (VBM) is set at 0 eV.

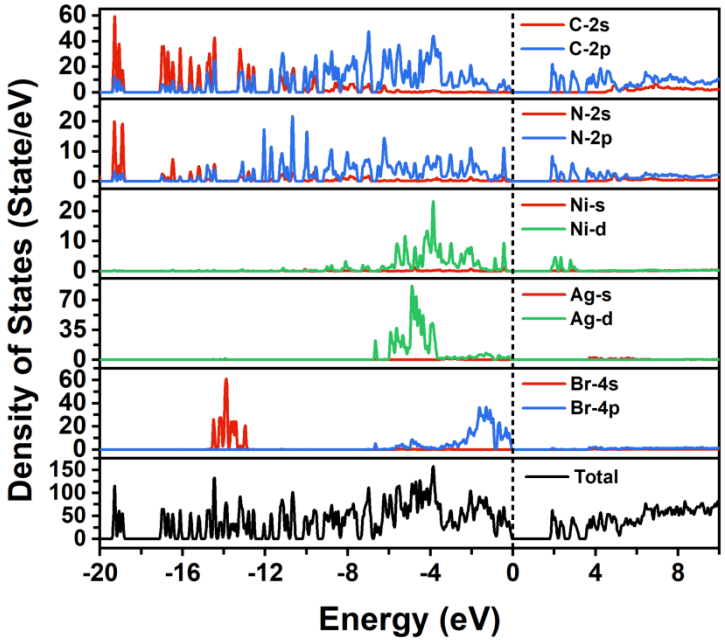

Fig. S14 The total density of states and partial density of states of compound **2**. The valence-band maximum (VBM) is set at 0 eV.

The DFT results of compound **1** were shown in Fig. S13. As can be seen, its CBM is primarily composed of the Co−3d, C−2p, and N−2p orbitals, while the I−5p and Co−3d states contribute mostly to the VBM near the Fermi level. In addition, the Ag−4d state appears in the range of −3 to −5 eV, and the region between −5 and −10 eV largely arises from the C−2p and N−2p orbitals.

Table S5 Summary of band gaps of representative hybrids in the literature.

Compound	Dimension	Space group	Band gap (eV)	Reference

$[Co(phen)_3]Ag_2I_4·3DMF$	0D	$P\bar{1}$	2.59	[1]
$[Ni(DMSO)_6][Ag_5I_7]$	1D	*Pbcm*	2.73	[2]
$[Fe(bipy)_3]AgBiI_6$	0D	$P2_1/c$	1.92	[3]
$[C_3H_9NI]_4AgBiI_8$	2D	$P\bar{1}$	1.87	[4]
$[PPh_4]_4Ag_2Bi_2I_{12}$	0D	*Pbca*	2.10	[5]
$[Me_3TPA][Ag_5I_8]$	1D	*Cc*	2.51	[6]
$[Co(phen)_3]_2Ag_{11}I_{15}·H_2O$	2D	*P*63/*m*	2.84	[7]
$K[Zn(bipy)_3]_2Ag_6Br_{11}$	2D	$R\bar{3}$	2.61	[8]
$[Zn(bipy)_3]_2Ag_{13}Br_{17}$	2D	*Pcca*	2.71	[8]
$[C_4H_{10}N]_4AgBiBr_8$	2D	*C*2/*m*	2.85	[9]
$[C_3H_9NCl]_4AgBiBr_8$	2D	*Pc*	2.69	[10]
$[Fe(bipy)_3]AgBiBr_6$	0D	*C*2/*c*	1.82	[3]
$[NH_4][Fe(bipy)_3]_2[Ag_6Br_{11}]$	2D	$R\bar{3}$	1.90	[11]
$[\{Cu(phen)\}_2(\mu\text{-}OH)_2(Ag_3Br_5)]_n$	1D	$P\bar{1}$	2.48	[12]
$[C_5H_{11}N_2]PbI_3$	1D	2.72	3.43	[13]
$[Ni(phen)_3]Pb_2I_6·CH_3CN$	1D	2.68	0.8	[14]
$[Co(bipy)_3][Pb_2Br_6CH_3OH]$	1D	3.04	0.66	[15]
$[Fe(bipy)_3]Pb_2Br_6$	1D	2.02	2.18	[15]
Cd(5-BIPA)(phen)	1D	NA	3.72	[16]
$CdCl_2(C_{13}H_9N)$	2D	NA	0.2596	[17]
$[NH_4][Co(2,2\text{-}bipy)_3]_2Ag_6I_{11}$	2D	$R\bar{3}$	1.75	This work
$[NH_4][Ni(2,2\text{-}bipy)_3]_2Ag_6Br_{11}$	2D	$R\bar{3}$	2.84	This work

6. References

[1] C. Y. Tang, J. Yao, Y. Y. Li, Z. R. Xia, J. B. Liu, C. Y. Zhang, *Inorg. Chem.*, 2020, **59**, 13962−13971.

[2] Y. Mu, D. Wang, X. D. Meng, J. Pan, S. D. Han, Z. Z. Xue, *Cryst. Growth Des.*, 2020, **20**, 1130−1138.

[3] B. Zhang, J. Li, M. Pang, Y. S. Wang, M. Z. Liu, H. M. Zhao, *Inorg. Chem.*, 2022, **61**, 406−413.

[4] Y. P. Yao, B. Kou, Y. Peng, Z. Y. Wu, L. N. Li, S. S. Wang, X. Y. Zhang, X. T. Liu, J. H. Luo, *Chem. Commun.*, 2020, **56**, 3206−3209.

[5] N. Dehnhardt, H. Borkowski, J. Schepp, R. Tonner, J. Heine, *Inorg. Chem.*, 2018, **57**, 633−640.

[6] M. Y. Xie, T. Liu, Y. Y. Xia, Q. Wei, S. D. Han, Z. Z. Xue, J. Pan, *Inorg. Chem.*, 2024, **63**, 23036−23043.

[7] T. L. Yu, Y. B. Fu, Y. L. Wang, P. F. Hao, J. J. Shen, Y. L. Fu, *CrystEngComm*, 2015, **17**, 8752−8761.

[8] C. Y. Yue, X. W. Lei, Y. F. Han, X. X. Lu, Y. W. Tian, J. Xu, X. F. Liu, X. Xu, *Inorg. Chem.*, 2016, **55**, 12193−12203.

[9] B. A. Connor, L. Leppert, M. D. Smith, J. B. Neaton, H. I. Karunadasa, *J. Am. Chem. Soc.*, 2018, **140**, 5235−5240.

[10] W. Q. Guo, X. T. Liu, S. G. Han, Y. Liu, Z. Y. Xu, M. C. Hong, J. H. Luo, Z. H. Sun, *Angew. Chem. Int. Ed.*, 2020, **59**, 13879−13884.

[11] B. Zhang, J. Li, X. Chen, M. F. Yang, H. Y. Shen, J. C. Zhu, *Inorg. Chem. Commun.*, 2022, **137**,

109250.
[12] Y. M. Tian, T. H. Ren, H. J. Zhu, D. X. Jia, *CrystEngComm*, 2024, **26**, 3911−3919.
[13] S. Y. Xie, J. T. Wu, B. H. Li, H. C. Liu, H. Wang, J. Li, B. Zhang, *Cryst. Res. Technol.*, 2024, **59**, 2400060.
[14] B. Zhang, H. Y. Sun, J. Li, Y. R. Xu, Y. P. Xu, X. Yang, G. D. Zou, *Dalton Trans.*, 2020, **49**, 1803−1810.
[15] Y. Q. Liu, S. Huang, J. D. Leng, W. Q. Lin, *Molecules*, 2024, **29**, 4217.
[16] X. G. Yang, Y. J. Chen, P. P. Yin, J. W. Diao, Y. Y. Cheng, L. F. Ma, *Inorg. Chem.*, 2023, **62**, 19389−19394.
[17] X. G. Yang, Y. J. Chen, P. P. Yin, Y. Li, S. Y. Yang, Y. M. Li, L. F. Ma, *Chem. Sci.*, 2024, **15**, 14202−14208.